Journal of Power Sources 189 (2009) 958–965

Contents lists available at ScienceDirect

Journal of Power Sources

journal homepage: www.elsevier.com/locate/jpowsour

Blended Nafion®/SPEEK direct methanol fuel cell membranes for reduced methanol permeability

Jie-Cheng Tsai, Hui-Pin Cheng, Jen-Feng Kuo, Yao-Hui Huang, Chuh-Yung Chen*

Department of Chemical Engineering, National Cheng-Kung University, Tainan 70148, Taiwan

ARTICLE INFO

Article history:
Received 18 November 2008
Received in revised form 16 December 2008
Accepted 17 December 2008
Available online 27 December 2008

Keywords:
Proton exchange membrane
Sulfonated poly(ether ether ketone)
Nafion®
Blend
Methanol permeability
Direct methanol fuel cell

ABSTRACT

Sulfonated poly(ether ether ketone)s (SPEEKs) were substituted on a polymer main chain that had previously been prepared by sulfonation of poly(ether ether ketone)s in concentrated sulfuric acid for a specified time. The product was then blended with Nafion® to create composite membranes. The blended SPEEK-containing membranes featured flaky domains dispersed in the Nafion® matrix. These blends possessed a high thermal decomposition temperature. Additionally, owing to the more crystalline, the blended membranes had a lower water uptake compared to recast Nafion®, the methanol permeability was reduced to 1.70×10^{-6} to 9.09×10^{-7} $cm^2\ s^{-1}$ for various SPEEK concentrations, and a maximum proton conductivity of ~0.050 S cm^{-1} was observed at 30 °C. The single-cell performances of the Nafion®/SPEEK membranes, with various SPEEK concentrations and a certain degree of sulfonation, were 15–25 mW cm^{-2} for SPEEK53 and 19–27 mW cm^{-2} for SPEEK63, at 80 °C. The power density and open circuit voltage were higher than those of Nafion® 115 (power density = 22 mW cm^{-2}). The blended membranes satisfy the requirements of proton exchange membranes for direct methanol fuel cell (DMFC) applications.

1. Introduction

Fuel cells convert chemical energy directly into electrical energy and are promising as alternative energy conversion devices. Direct methanol fuel cells (DMFCs) have attracted significant attention because of their highly efficient energy conversion, low environmental emissions, simple structural design, convenient fuel storage and possible use in transportation scenarios [1]. DMFCs are suitable for both stationary and portable devices, such as cell phones and laptop computers [2].

The proton exchange membrane is one of the key components in a fuel cell system. Perfluorosulfonic acid membranes, such as Nafion® with fluoroalkyl ether side chains and sulfonic acid end groups, are the most commonly used due to their high electrochemical stability, mechanical strength and proton conductivity [3]. However, avoiding high methanol crossover in commercial Nafion® membranes is a major technical challenge. Methanol is easily transported from the anode to the cathode side of the cell, where it is oxidized without any contribution to power generation [4]. The undesirable crossover of methanol reduces fuel efficiency and causes a significant loss of performance due to catalyst poisoning and an increase of overpotential at the cathode [5].

Over the past few years, in order to overcome the problem of methanol crossover, many new materials have been investigated via two general approaches: (a) synthesis of new polymers, including sulfonated poly(ether ether ketone) [6], polysulfone [7], and polyimide [8], and (b) modification of existing polymers by introduction of a methanol barrier component. These modifications include incorporation of inorganic particles (e.g., silicon oxide [9], titanium oxide [10], zeolites [11] and montmorillonite clay [12]) into Nafion®, and blending poly(vinylidene fluoride) [13], poly(vinyl alcohol) [14], poly(1-vinylimidazole) [15], polypyrrole [16], and polybenzimidazile [17] with Nafion®. Unfortunately, reduction of methanol permeability is always accompanied by a significant decrease in proton conductivity. Understanding the relationship between the microstructure (i.e., diameter of proton transfer channels, size of ionic clusters, etc.) and the associated transport properties may help us optimize proton-exchange membranes [18]. It is known that methanol passes through these membranes primarily via ionic channels. Thus, methanol permeability is determined by the diameter of these channels and the sizes of ionic clusters, which are mainly dependent upon the ability of the membrane to swell [19]. It should be possible to reduce swelling by adjusting the microstructure of the membrane.

SPEEKs have been extensively studied and tested for fuel cell applications. SPEEK membranes possess many good attributes, such as low methanol permeability, good mechanical properties, high heat distortion temperature, and good processing capacity. In this study, blended membranes consisting of Nafion® and small

* Corresponding author. Tel.: +886 6 2757575x62643; fax: +886 6 2360464.
E-mail address: ccy7@ccmail.ncku.edu.tw (C.-Y. Chen).

0378-7753/$ – see front matter © 2008 Elsevier B.V. All rights reserved.
doi:10.1016/j.jpowsour.2008.12.071

amounts of SPEEKs were prepared using a simple, inexpensive process to reduce swelling, methanol crossover and cost, while maintaining good proton conductivity by adjusting the microstructure of the membrane. Moreover, the thickness of a low methanol crossover membrane would have to be reduced in order to minimize membrane resistance losses in a fuel cell. The novel Nafion®/SPEEK composite membranes described here are thinner than Nafion® 115. The composite membranes demonstrate reduced swelling and methanol permeability, compared with Nafion® membranes alone, with improvement of DMFC performance.

2. Experimental details

2.1. Materials and experimental procedure

2.1.1. Materials

PEEK 450G Victrex® was obtained from ICI Co. and was used as received. Nafion® 115 and Nafion® solution (5 wt.%, sulfonic acid form) in a 1-propanol/ethanol/water mixture were purchased from E.I. Dupont de Nemours & Co. Concentrated sulfonic acid (95–98%) was purchased from Aldrich Chemical Co. Dimethylacetamide (DMAc) and methanol were purchased from Mallinckrodt Co. Nafion® 115 was treated to completely remove all impurities by boiling in 3% H_2O_2, 0.5 M H_2SO_4 and then adding deionized water.

2.1.2. Polymer sulfonation

Initially, 5 g of PEEK was sulfonated in 150 mL of concentrated sulfuric acid at room temperature under vigorous mechanical stirring [1,20,21] for a specified time. The resulting sulfonated polymer solution (SPEEK) was decanted into a large excess of ice-cold water. The precipitated polymer was filtered and washed repeatedly with deionized water until the pH was neutral, then dried under vacuum at 100 °C for 24 h. In this study, the degree of sulfonation was determined to be 0.53 (SPEEK53) and 0.63 (SPEEK63).

2.1.3. Membrane preparation

The composite membranes were prepared by blending Nafion® and the prepared SPEEK. The Nafion® solution was evaporated to dryness, and then Nafion® and SPEEK were separately dissolved in DMAc to obtain a 15 wt.% solution. The SPEEK solution was added to the Nafion® solution at room temperature under vigorous stirring. The weight ratios of the blends varied from 0.5% to 3% SPEEK. The mixtures were cast onto glass dishes and dried under vacuum at 80 °C. Finally, the cast membranes were dried at 120 °C for 2 h, at which point a thickness of $\sim 100 \pm 10\,\mu m$ was measured. The blended membranes were stored in deionized water. Moreover, the recast Nafion® was prepared by Nafion® solution with a thickness of $\sim 100 \pm 10\,\mu m$ which was used to compare the properties and DMFCs performance, and the commercial Nafion® 115 was used to only compare the DMFCs performance in this study.

2.2. Proton nuclear magnetic resonance (^{1}H NMR)

The SPEEK spectra were obtained in DMSO-d_6 solution (10 wt.%) at room temperature. The ^{1}H NMR spectra were obtained with a Varian Unity 600 spectrometer and a Bruker AMX 600 MHz spectrometer.

2.3. Fourier transform infrared spectroscopy (FT-IR)

An FT-IR spectrometer with an attenuated total reflection (ATR) attachment was used to identify the functional groups present within the membranes. Spectra were obtained with a Bio-Rad FTS-40A spectrometer over the wavelength range 700–4000 cm^{-1}. Each spectrum is the average of 48 scans with a resolution of 4 cm^{-1}.

2.4. Scanning electron microscopy (SEM)

All of the specimens were sputter-coated with Pt for 120 s. The membranes were freeze-fractured to reveal the cross-sectional area and the morphology was examined using a Hitachi S4200 field emission scanning electron microscope.

2.5. Wide-angle X-ray diffraction (WAXD)

WAXD was performed with a conventional wide-angle X-ray diffractometer (Philips Electronics) using a CuKα source. The blended membranes were scanned at up to 60 s per 4° angular step.

2.6. Thermogravimetric analysis (TGA)

All membranes were heated at 120 °C for 30 min in a furnace to remove moisture. The dynamic TGA experiments were performed under a nitrogen atmosphere with a TGA Q50 thermal analyzer (TA Instruments, WI) from 100 °C to 700 °C at a heating rate of 20 °C min^{-1}.

2.7. Differential scanning calorimetry (DSC)

A Dupont DSC 2910 differential scanning calorimeter was used to analyze the thermal transition behavior of the blended membranes from 30 °C to 250 °C at a heating rate of 10 °C min^{-1} under nitrogen atmosphere.

2.8. Water uptake by membranes

Membranes were dried under vacuum at 120 °C to a constant weight. The water uptake was measured by immersing the membranes in deionized water and heating from 30 °C to 80 °C.

The weight of equilibrium water uptake was determined as:

$$\text{Water uptake} = \frac{W_{\text{wet}} - W_{\text{dry}}}{W_{\text{dry}}} \times 100\% \quad (1)$$

where W_{wet} and W_{dry} are the weights of the wet and dry membrane, respectively.

2.9. Methanol permeability

The methanol permeabilities of the membranes were determined using a diaphragm diffusion cell. The membranes were equilibrated in deionized water overnight with stirring. The initial concentration of methanol in one side of the cell (compartment A) was 2 M, while the other side of the cell (compartment B) contained deionized water. The increase in methanol concentration over time was determined by gas chromatography. The methanol permeability was calculated from the slope of a least-squares linear regression:

$$C_B(t)\frac{A}{V_B}\frac{P}{L}C_A(t - t_0) \quad (2)$$

where A is the effective membrane area, L is the membrane thickness, C_A and C_B are the initial concentrations of methanol in compartments A and B, respectively, and V_B is the volume of compartment B.

2.10. Proton conductivity measurement

The proton conductivity cell was immersed in water at a constant temperature that was preselected from the range 30 °C to 80 °C. The in-plane conductivities of the blended membranes were determined with an electrochemical cell. Stainless steel blocking electrode was used for the measurement. AC impedance analysis

was performed with Autolab PGSTAT 30 equipment (Eco Chemie B.V., Netherlands). The frequency response analysis (FRA) software used an oscillation potential of 10 mV from 100 kHz to 10 Hz. The proton conductivities of the membranes were determined as follows:

$$\sigma = \frac{l}{RA} \tag{3}$$

where σ is the proton conductivity, l is the distance between the electrodes, R is the membrane resistance obtained by impedance analysis, and A is the membrane area.

2.11. Single-cell performance

Nafion® 115, recast Nafion® and the prepared membrane blends were used as proton exchange membranes in fuel cells, and the catalysts for the anode and the cathode were applied to carbon paper by spreading. The anode and cathode consisted of commercial 20 wt.% Pt/Ru (1:1) in Vulcan carbon (E-TEK) with Pt loading of 1.2 mg cm^{-2} and 0.6 mg cm^{-2}, respectively. Methanol (2 M) was supplied to the anode with a micro-pump at 2 mL min^{-1}, while the cathode was supplied with dry oxygen at a rate of 100 mL min^{-1}. Single-cell performance was evaluated using a DMFC unit with a cross-sectional area of 4 cm^2.

3. Results and discussion

3.1. Polymer characteristics

^{1}H NMR spectroscopy was used to provide chemical characterization, and to determine the degree of sulfonation. Fig. 1 shows the ^{1}H NMR spectrum of SPEEK dissolved in DMSO-d_6. All characteristic peaks of H_a and $H_{a'}$ protons appeared at low field. The H_b and $H_{b'}$ protons were located at 7.14 ppm and 7.00 ppm, respectively. The $H_{c'}$ protons of the unsubstituted hydroquinone ring appeared as a characteristic singlet at 7.25 ppm. The sulfonic groups were introduced into the hydroquinone ring and caused a significant downfield shift of the H_c, H_d, and H_e signals in the hydroquinone ring at 7.20 ppm, 7.09 ppm, and 7.50 ppm, respectively [22,23]. The degree of substitution was derived from the ratio between the peak area of the H_e signal and the integrated peak area of the signals corresponding to the other aromatic hydrogen atoms. In this study, the degree of sulfonation was determined to be 0.53 (SPEEK53) and 0.63 (SPEEK63).

The FT-IR ATR spectra of dried recast Nafion® and Nafion®/SPEEK are shown in Fig. 2. In the SPEEK spectrum, the aromatic C—C band

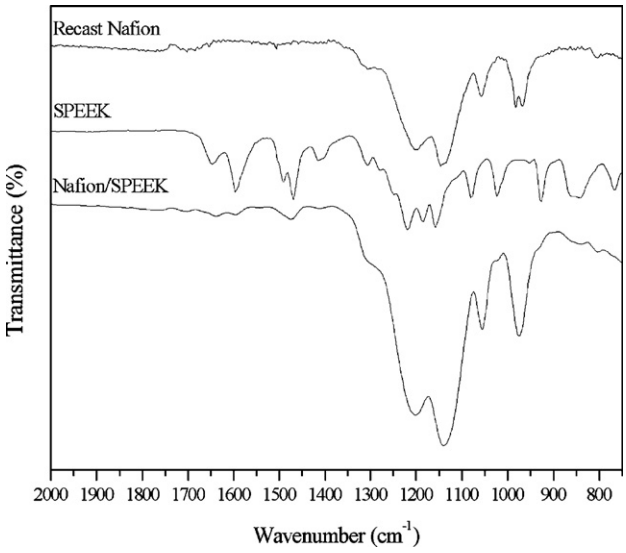

Fig. 2. The FT-IR ATR spectra of recast Nafion® and Nafion®/SPEEK.

was observed to split into two peaks, 1470 cm^{-1} and 1493 cm^{-1}, due to the sulfonation-induced substitution. The absorption peak at 1022 cm^{-1} was associated with S=O stretching vibration. The absorption peaks at 1080 cm^{-1} and at 1250 cm^{-1} can be associated with the symmetrical O=S=O stretching vibration, and the asymmetric stretching vibration of the sulfonic groups, respectively. The absorption at 1651 cm^{-1} was associated with the backbone carbonyl stretching band [23,24]. In the blended membranes, Fig. 2 shows that the peaks at 1200 cm^{-1} and at 1144 cm^{-1} were associated with the asymmetric and the symmetric F—C—F stretching vibration, respectively. Bands at 1410 cm^{-1} and 851 cm^{-1} were connected with S=O and S—OH stretching of the—SO_3H group, while 1052 cm^{-1} was linked to the symmetric —SO_3^- stretching vibration [25].

3.2. Morphology

SEM was used to study the morphology of the recast Nafion® and blended membranes. SEM micrographs showing the freeze-fractured cross-sectional morphologies of the recast Nafion® and blended membranes with various SPEEK content levels are shown in Fig. 3(a–g). The recast Nafion® and SPEEK appear to be incompatible with each other. The SPEEK seemed to form a dispersive phase,

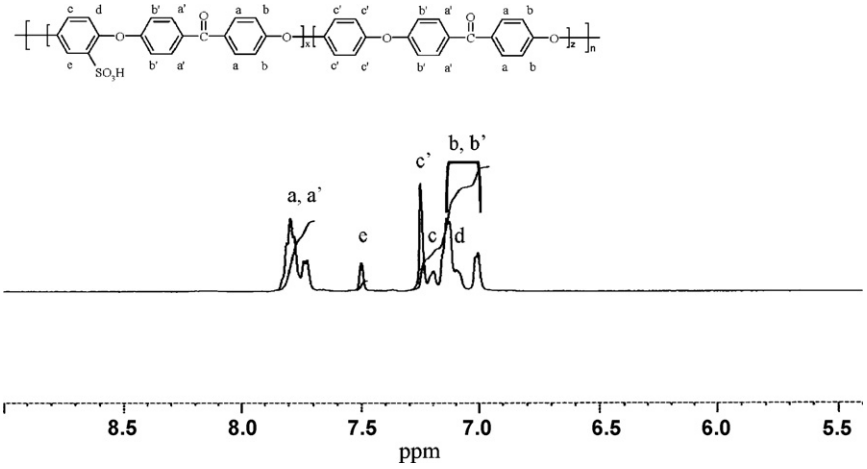

Fig. 1. The ^{1}H NMR spectrum for SPEEK.

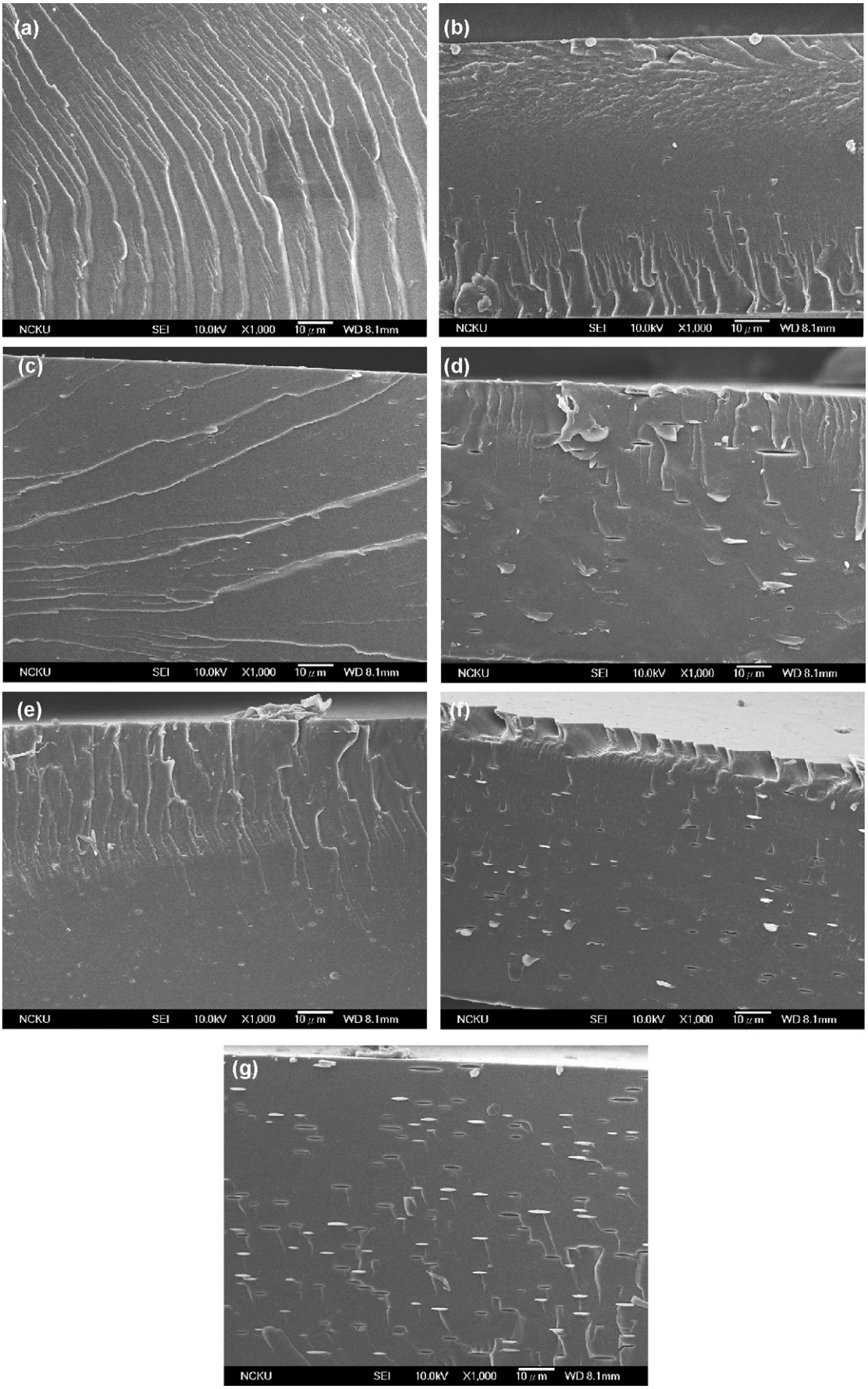

Fig. 3. The SEM images of (a) Recast Nafion®, (b) Nafion®/SPEEK53-0.5, (c) Nafion®/SPEEK53-1, (d) Nafion®/SPEEK53-3, (e) Nafion®/SPEEK63-0.5, (f) Nafion®/SPEEK63-1, and (g) Nafion®/SPEEK63-3.

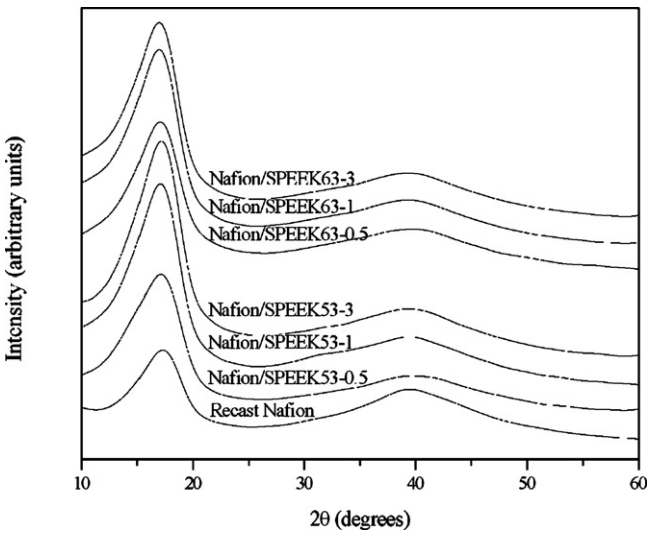

Fig. 4. The WAXD spectra of recast Nafion® and Nafion®/SPEEK.

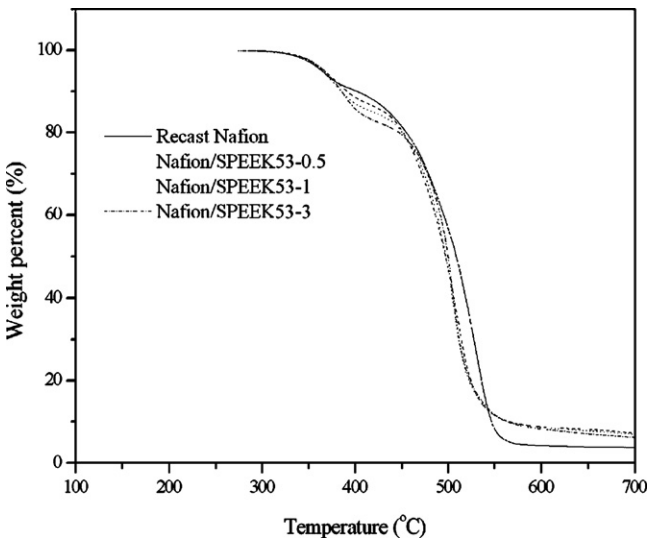

Fig. 5. The thermogravimetric curves of recast Nafion® and Nafion®/SPEEK.

appearing as "flakes" in the Nafion® matrix. The size of these flake-like domains increased with increasing SPEEK content and showed highly oriented domains that paralleled the substrate.

Nafion® is a semi-crystalline polymer and blending it with other polymers could affect its crystallinity. Nafion® is known to have a weak WAXD reflection at 18° due to the (1 0 0) plane of the crystalline PTFE backbone. This peak at $2\theta = 39°$ is on the order of the distance between the nearest neighbor CF_2 units [26]. Fig. 4 shows a comparison of the WAXD spectra for recast Nafion® and blended membranes. Both recast Nafion® and the blended membranes showed a crystalline reflection which was superimposed as a shoulder on a large amorphous halo. Unfortunately, the superposition of the sharp crystalline peak and the broad amorphous halo by the low level of crystallinity in the Nafion® and SPEEK made it impossible to separate and qualitatively analyze. However, full width at half maximum (FWHM) of the blended membranes decreased with increasing SPEEK content, indicating that the perfection of the crystallites in the membranes became high gradually. Furthermore, SPEEK can induce bigger crystallite size in the membranes. The morphology affected the formation of ionic domains and ultimately impacted the hydration and conduction of ions through the membranes [27].

3.3. Thermal characteristics

The thermal stability of the recast Nafion® and the blended membranes were investigated using TGA. The influence of SPEEK blending on the 5 wt.% loss temperature (T_{d5}) is shown in Fig. 5. Nafion® is known to be a thermally stable membrane, and has a T_{d5} of 364 °C. According to literature [3], thermogravimetric curves recorded under nitrogen atmospheres are characterized by four steps: (i) gradual loss of water from 25 to 290 °C; (ii) desulfonation accompanied by decomposition of the ether groups on the side chains from 290 °C to 400 °C; (iii) side chain decomposition from 400 °C to 470 °C; and (iv) degradation of the PTFE backbone from 470 °C to 560 °C. In all of the blended membranes, T_{d5} was approximately 367 °C for various contents of SPEEK53 and SPEEK63, which was closed to the recast Nafion® (364 °C).

DSC analysis was used to characterize the thermal transition of the recast Nafion® and blended membranes. Fig. 6 shows that two transition temperatures were present in the DSC curves of the recast Nafion® and the blended membranes. In recast Nafion®, the first endothermic peak appeared at about 110 °C, which may be interpreted as the cluster transition temperature. The second peak was a weak, broad endothermic peak at around 200 °C, which was assigned as the melting peak of the non-polar crystallite backbone [28]. With the introduction of SPEEK into the Nafion® membrane, the cluster transition temperature increased with increasing SPEEK content and with increasing degree of sulfonation. In the blended membranes, the cluster transition temperature increased to 73 °C, 94 °C, and 136 °C for 0.5%, 1%, and 3% SPEEK53, respectively, and to 73 °C, 134 °C, and 138 °C for 0.5%, 1%, and 3% SPEEK63, respectively. The increase of cluster transition temperatures compared with recast Nafion® was verified only for 3% of SPEEK53 and 1–3% of SPEEK63. The shift in this peak was strongly related to crystallization which hindered the transition of cluster and was consistent with the observed WAXD results.

3.4. Water uptake

It is well-known that the proton conductivity and methanol permeability of membranes are strongly related to the presence of water. An adequate level of water uptake is needed to maintain good proton conductivity; however, water uptake should be minimized to ensure low methanol permeability. Consequently, maintaining

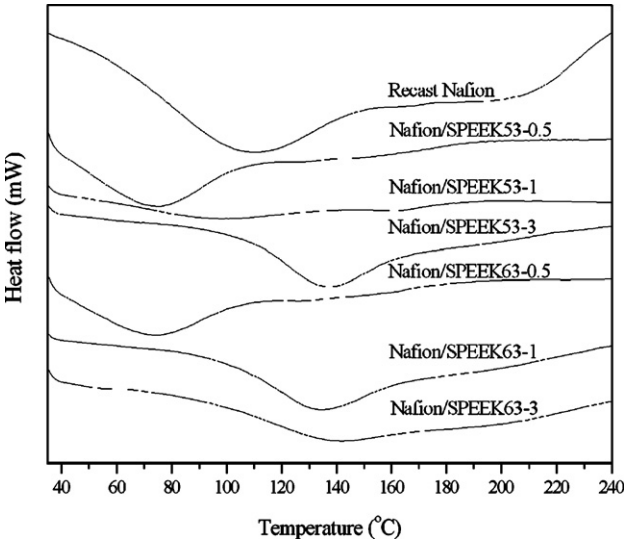

Fig. 6. The transition temperature of recast Nafion® and Nafion®/SPEEK.

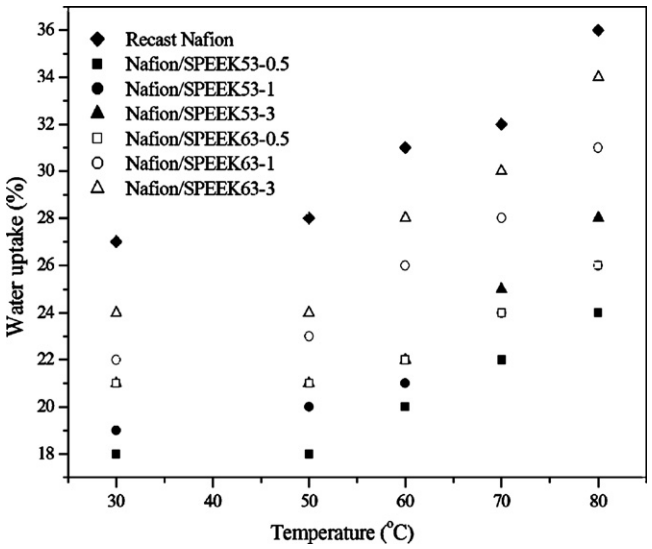

Fig. 7. The water uptake of recast Nafion® and Nafion®/SPEEK.

the appropriate level of water uptake is very important to the ultimate performance. The native SPEEK showed a relatively high water uptake of 31% and 38% for SPEEK53 and SPEEK63, respectively, compared with recast Nafion® at 30 °C. Fig. 7 shows the water uptake of the blended membranes as a function of temperature. The water uptake increased with increasing SPEEK content. At temperatures of up to 80 °C, the water uptake increased sharply to 24%, 26%, and 28% for 0.5%, 1%, and 3% SPEEK53, respectively, and to 26%, 31%, and 34% for 0.5%, 1%, and 3% SPEEK63, respectively. This was perhaps due to the formation of ionic clusters. When the temperature and the degree of sulfonation were high, the dispersed sulfonic groups readily formed ion domains, which are hydrophilic and predominantly responsible for water uptake [29]. Furthermore, the water uptake of the blended membranes was 18–24% at 30 °C, compared with 27% for recast Nafion®, although the water uptake of native SPEEK was higher than that of recast Nafion®. The introduction of SPEEK allowed for adjustment of the diameter of transfer channels and the size of ionic clusters in the crystalline microstructure.

3.5. Methanol permeability

The methanol permeability of native SPEEK membranes increased with increasing degree of sulfonation from 3.14×10^{-7} cm^2 s^{-1} to 3.44×10^{-7} cm^2 s^{-1} for SPEEK53 and SPEEK63, respectively. These values were all lower than that of recast Nafion® (2×10^{-6} cm^2 s^{-1}). The sulfonic groups aggregate to form ion clusters in the presence of water that further interconnect the hydrophilic domains within the membrane. This tendency to absorb water plays a major role in the transport of methanol through the membrane by hydration of the ionizable sulfonic groups. The methanol permeability of the blended membranes was less than that of recast Nafion®. The methanol permeabilities of the blended membranes decreased with increasing SPEEK content, with relatively low methanol permeabilities of 1.50×10^{-6} cm^2 s^{-1}, 1.16×10^{-6} cm^2 s^{-1}, and 9.09×10^{-7} cm^2 s^{-1} for 0.5%, 1%, and 3% SPEEK53 content, respectively, and 1.70×10^{-6} cm^2 s^{-1}, 1.40×10^{-6} cm^2 s^{-1}, and 1.27×10^{-6} cm^2 s^{-1} for 0.5%, 1%, and 3% SPEEK63 content, respectively, at 30 °C. This demonstrates a reduction in methanol crossover following the introduction of SPEEK into the Nafion® membrane. Changes in the methanol permeability and water uptake of the blended membranes were similar. This reduction in methanol crossover is favorable for DMFC applications.

3.6. Proton conductivity

In general, high proton conductivity and low methanol crossover are required for superior DMFC performance. The proton conductivity of the blended membranes from 30 °C to 80 °C increased to 0.045–0.079 S cm^{-1}, 0.042–0.078 S cm^{-1}, and 0.041–0.077 S cm^{-1} for 0.5%, 1%, and 3% SPEEK53 content, respectively, and 0.052–0.099 S cm^{-1}, 0.047–0.097 S cm^{-1}, and 0.042–0.089 S cm^{-1} for 0.5%, 1%, and 3% SPEEK63 content, respectively. Proton transport in membranes requires well-connected channels formed by ionic clusters of hydrophilic sulfonic groups. Aggregation of these ionic domains was observed with increasing temperature, leading to formation of the percolation of ionic channels with good connectivity, which allowed for rapid transport of protons. By contrast, it was apparent that the higher degree of sulfonation increased the proton conductivity at the same SPEEK content level. The proton conductivity of the blended membranes decreased with increasing SPEEK content. These values were lower than that of recast Nafion® (0.093 S cm^{-1}) measured at 30 °C. It is likely that the crystallinity and lower conductivity of SPEEK caused a decrease in proton conductivity.

The activation energy (E_a), the minimum energy required for proton transport across the membrane, was calculated by fitting to the Arrhenius equation:

$$\sigma = A \times e^{-E_a/RT} \quad (4)$$

where σ is the proton conductivity (S cm^{-1}), E_a is the activation energy (kJ mol^{-1}), R is the universal gas constant (8.314 J mol^{-1} K^{-1}), and T is the absolute temperature (K). Fig. 8 shows the Arrhenius plots for recast Nafion® and the blended membranes. All blends showed linear Arrhenius behavior between 30 °C and 80 °C. Recast Nafion® and the blended membranes had activation energies of 8.14 kJ mol^{-1} and 9.88–13.61 kJ mol^{-1}, respectively. In general, the proton conductive mechanism in these membranes is well known to occur by two routes [30]: (i) the first route is a hopping or jumping mechanism, also known as the Grotthuss model, wherein a proton is passed down through a channel of water molecules. The protons are transferred from one vehicle to another by hydrogen bonds; (ii) the second route is a vehicle mechanism, wherein a proton combines with solvent molecules, producing a complex like H_3O^+, $H_5O_2^+$, $H_7O_3^+$ or $CH_3OH_2^+$ or some similar complex. This complex then diffuses through the membrane.

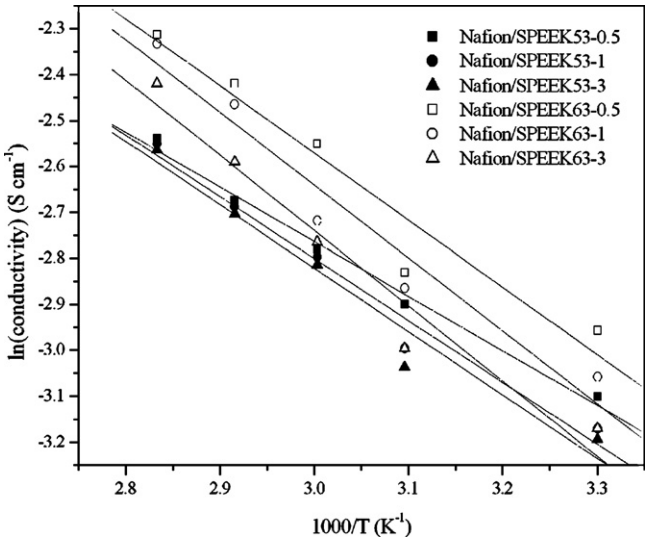

Fig. 8. Arrhenius plots of proton conductivity for Nafion®/SPEEK.

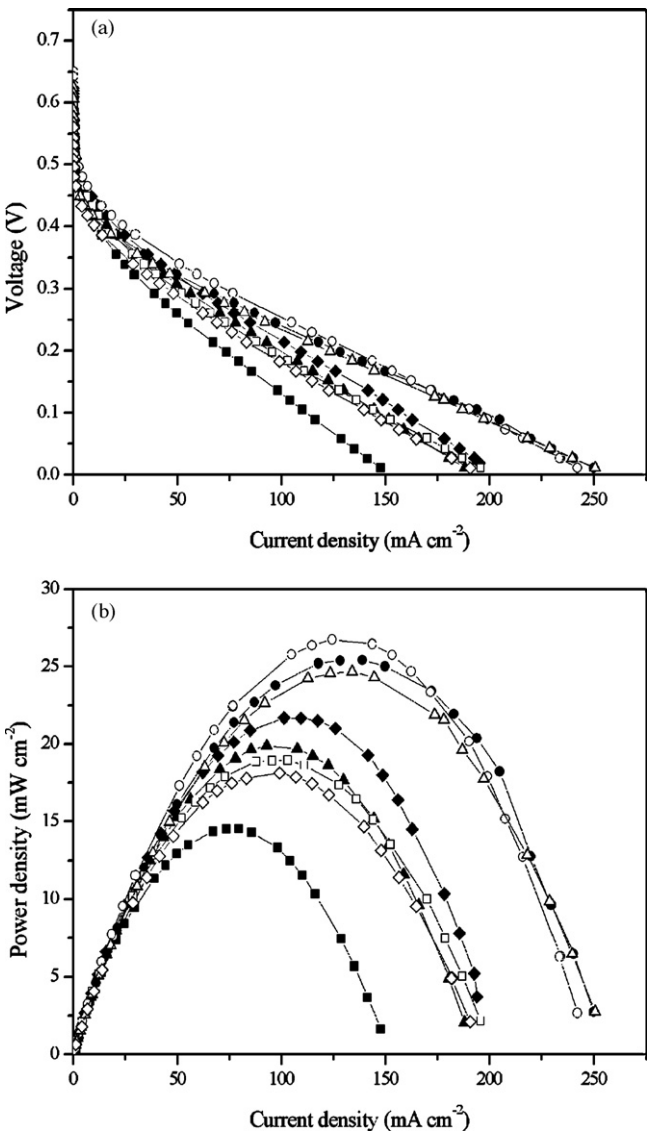

Fig. 9. The performance curves of Nafion® and blended membranes: (a) Polarization curve: (♦) Nafion® 115, (◊) Recast Nafion®, (■) Nafion®/SPEEK53-0.5, (●) Nafion®/SPEEK53-1, (▲) Nafion®/SPEEK53-3, (□) Nafion®/SPEEK63-0.5, (○) Nafion®/SPEEK63-1, and (△) Nafion®/SPEEK63-3. (b) Power density curve: (♦) Nafion® 115, (◊) Recast Nafion®, (■) Nafion®/SPEEK53-0.5, (●) Nafion®/SPEEK53-1, (▲) Nafion®/SPEEK53-3, (□) Nafion®/SPEEK63-0.5, (○) Nafion®/SPEEK63-1, and (△) Nafion®/SPEEK63-3.

3.7. Single-cell performance

The Nafion® 115 and blended membranes were then tested in DMFCs. Fig. 9 shows the performance results in terms of (a) polarization and (b) power density as a function of current density for various SPEEK contents. All characteristic curves displayed similar polarization behavior. In the region of low current density, activation control caused a large drop in potential, which decreased further for intermediate current densities, due to the intrinsic ohmic resistance. Although all contribute to a lower output upon applying a load to the system, only methanol crossover actively decreases the open circuit voltage. Nafion® 115 has a thickness of 127 μm, while the blended membranes are around 100 μm. In theory, Nafion® 115 is preferred in DMFCs because of its thickness: thicker membranes assure limited methanol crossover. However, in Fig. 9, single cells prepared with each of the blended membranes exhibited higher open circuit voltages (0.559–0.650 V) than Nafion® 115 (0.571 V) at 2 M methanol. This clearly indicates that the introduction of SPEEK significantly decreased the rate of methanol crossover in DMFCs, due to the relatively low methanol permeability. Although the conductivity of the blended membranes was lower than that of Nafion®, the DMFC performance can be improved by a reduction in methanol crossover and thickness. The blended membrane with 1% SPEEK63 content had the highest power density (27 mW cm^{-2}), which was better than that of the other blended membranes and Nafion® 115 (22 mW cm^{-2}). As the SPEEK content of blended membranes increased to 3%, the ohmic resistance increased and the performance decreased. As shown in Fig. 8, the performance of the single-cell improved with increasing degree of sulfonation for the same SPEEK content, due to higher proton conductivity. The maximum power density of blended membranes with various SPEEK contents occurred at a degree of sulfonation of 15–25 mW cm^{-2} for SPEEK53 and 19–27 mW cm^{-2} for SPEEK63 at 80 °C.

4. Conclusion

In this study, SPEEK and Nafion® were used to prepare blended membranes. SPEEK was easy to prepare and was blended with Nafion® using a low-cost process. The blended membranes were characterized using ^{1}H NMR, FT-IR ATR, SEM, WAXD, TGA, DSC, water uptake, methanol permeability, conductivity, and single-cell performance. ^{1}H NMR revealed that the degrees of sulfonation of the prepared SPEEKs were 0.53 and 0.63, and FT-IR ATR confirmed the composition of the blended membranes. The introduction of SPEEK caused the blended membranes to be more crystalline and showed a "flaky" dispersive phase in the Nafion® matrix. The resulting crystalline microstructure of the membranes decreased the methanol permeability, suppressed methanol crossover, decreased the water uptake, and maintained reasonable thermal properties. Although the conductivity decreased for the blended membranes, we propose that the DMFC performance can be improved in the future by reducing methanol crossover levels. The blended membranes exhibited higher open circuit voltages and superior single-cell performance compared with that of Nafion® 115. The observed low methanol permeability and promising single-cell performance suggest that Nafion®/SPEEK-blended membranes warrant serious consideration for use in future DMFC applications.

Acknowledgements

The authors are extremely grateful to Ms. P.Y. Lin and Professor W.H. Lai for their crucial contribution to the ^{1}H NMR experiments and the single-cell performance test.

References

[1] S. Xue, G. Yin, Polymer 47 (2006) 5044–5049.
[2] Y.Z. Fu, A. Manthiram, M.D. Guiver, Electrochem. Solid-State Lett. 10 (2007) B70–B73.
[3] S. Tan, D. Belanger, J. Phys. Chem. B 109 (2005) 23480–23490.
[4] R. Wycisk, J. Chisholm, J. Lee, J. Lin, P.N. Pintauro, J. Power Sources 163 (2006) 9–17.
[5] F. Liu, C.Y. Wang, J. Electrochem. Soc. 154 (2007) B514–B522.
[6] P. Xing, G.P. Robertson, M.D. Guiver, S.D. Mikhailenko, S. Kaliaguine, Macromolecules 37 (2004) 7960–7967.
[7] N.Y. Arnett, W.L. Harrison, A.S. Badami, A. Roy, O. Lane, F. Cormer, L. Dong, J.E. McGrath, J. Power Sources 172 (2007) 20–29.
[8] N. Asano, M. Aoki, S. Suzuki, K. Miyatake, H. Uchida, M. Watanabe, J. Am. Chem. Soc. 128 (2006) 1762–1769.
[9] D.H. Jung, S.Y. Cho, D.H. Peck, D.R. Shin, J.S. Kim, J. Power Sources 106 (2002) 173–177.
[10] V. Baglio, A. Di Blasi, A.S. Arico, V. Antonucci, P.L. Antonucci, F.S. Fiory, S. Licoccia, E. Traversa, J. New Mater. Electrochem. Syst. 7 (2004) 275–280.
[11] V. Tricoli, F. Nannetti, Electrochim. Act. 48 (2003) 2625–2633.
[12] D.H. Jung, S.Y. Cho, D.H. Peck, D.R. Shin, J.S. Kim, J. Power Sources 118 (2003) 205–211.

[13] F.A. Landis, R.B. Moore, Macromolecules 33 (2000) 6031–6041.
[14] N.W. DeLuca, Y.A. Elabd, J. Power Sources 163 (2006) 386–391.
[15] B. Bae, H.Y. Ha, D. Kim, J. Electrochem. Soc. 152 (2005) A1366–A1372.
[16] H.S. Park, Y.J. Kim, W.H. Hong, Y.S. Choi, H.K. Lee, Macromolecules 38 (2005) 2289–2295.
[17] L. Gubler, D. Kramer, J. Belack, O. Unsal, T.J. Schmidt, G.G. Scherer, J. Electrochem. Soc. 154 (2007) B981–B1372.
[18] M.S. Kang, J.H. Kim, J. Won, S.H. Moon, Y.S. Kang, J. Membr. Sci. 247 (2005) 127–135.
[19] K.D. Kreuer, J. Membr. Sci. 185 (2001) 29–39.
[20] A. Carbone, R. Pedicini, G. Portale, A. Longo, L. D'Ilario, E. Passalacqua, J. Power Sources 163 (2006) 18–26.
[21] J.K. Lee, W. Li, A. Manthiram, J. Power Sources 163 (2008) 56–62.
[22] C. Bailly, D.J. Williams, F.E. Karasz, W.J. MacKnight, Polymer 28 (1987) 1009–1016.
[23] P. Xing, G.P. Robertson, M.D. Guiver, S.D. Mikhailenko, K. Wang, S. Kaliaguine, J. Membr. Sci. 229 (2004) 95–106.
[24] V.V. Lakshmi, V. Choudhary, I.K. Varma, Macromol. Symp. 210 (2004) 21–29.
[25] J. Hu, V. Baglio, V. Tricoli, A.S. Arico, V. Antonucci, J. Appl. Electrochem. 38 (2008) 543–550.
[26] K.Y. Cho, H.Y. Jung, K.A. Sung, W.K. Kim, S.J. Sung, J.K. Park, J.H. Choi, Y.E. Sung, J. Power Sources 159 (2006) 524–528.
[27] C. Zaluski, G. Xu, Macromolecules 27 (1994) 6750–6754.
[28] Y.F. Lin, Y.H. Hsiao, C.Y. Yen, C.L. Chiang, C.H. Lee, C.C. Huang, C.C.M. Ma, J. Power Sources 172 (2007) 570–577.
[29] S. Zhong, C. Liu, Z. Dou, X. Li, C. Zhao, T. Fu, H. Na, J. Membr. Sci. 285 (2006) 404–411.
[30] R.K. Nagarale, G.S. Gohil, V.K. Shahi, J. Membr. Sci. 280 (2006) 389–396.